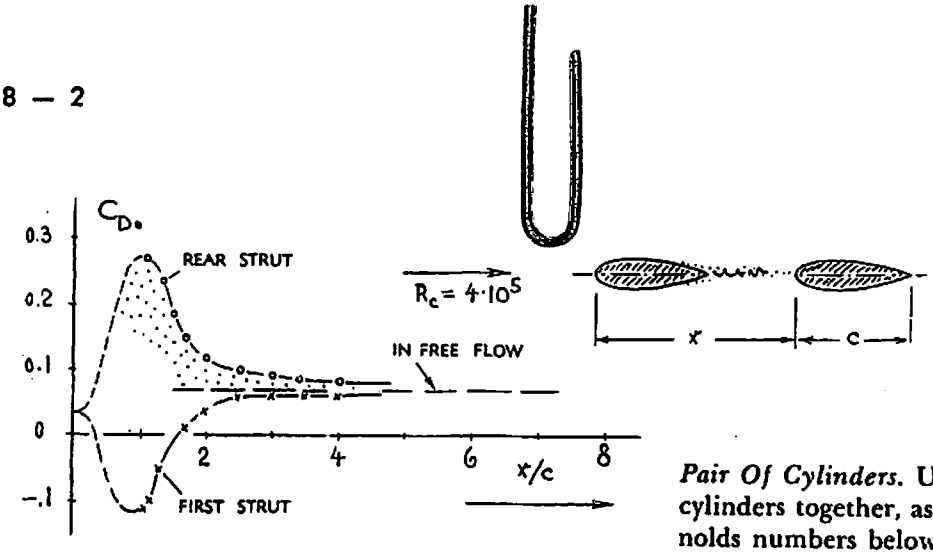


Figure 3. Drag of a pair of strut sections, one behind the other, in tandem (2,a).

Tandem Struts. Interference between the two struts in *figure 3* is basically different from that of the bluff bodies, considered so far. The drag of the rear section is increased (up to fourfold at $x/c \approx 1$). We have to assume that the flow separates from the rear of the second strut because of the momentum deficiency within the wake coming from the first strut. The fact that the drag of the first section is decreased is explained (2) by increased static pressure between the two struts pushing the first one forward, so to speak.

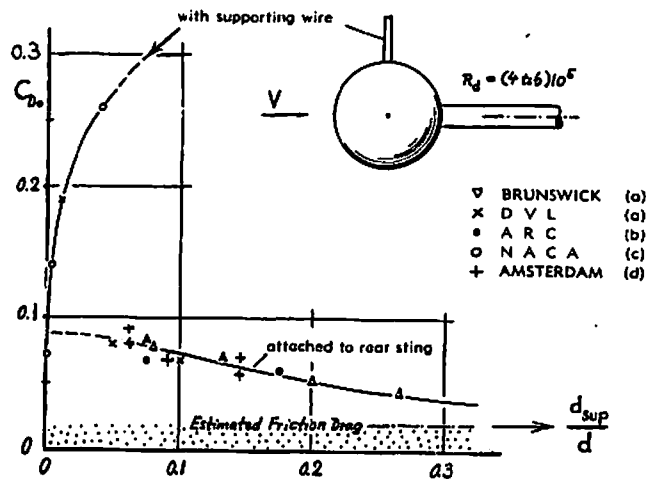


Figure 4. Drag of spheres at supercritical Reynolds numbers, affected by the presence of supporting devices (3).

Sting Support. Examples of favorable interference by placing one solid behind another one, are given in the "pressure drag" chapter (splitter plate and similar devices in figure 3-8). Another example is shown in *figure 4*. A "sting", supporting a sphere (tested at Reynolds numbers above transition), fills out the space of the wake, so to speak. As the diameter of this sting is increased, the flow attaches more and more completely to the rear of the body. The final drag coefficient, estimated to be in the order of 0.02, merely represents the skin-friction drag of the sphere.

Pair Of Cylinders. Upon bringing a pair of circular cylinders together, as in *figure 5*, their drag (at Reynolds numbers below transition) increases somewhat upon reducing the clearance distance to $y/d = 1$. Below this distance, the pattern of the vortex street switches from that of a pair (originating separately from each cylinder) to a combined system (2,b). Note that the Strouhal number (see page 3-6) reduces from "S" = 0.21 to ≈ 0.10 at $y/d \rightarrow$ zero. Upon referring the frequency of the pair of cylinders to their combined "height" of "2 d", the "0.1" transforms into "0.2" as approximately for a single cylinder. The graph also shows that the drag coefficient passes through a minimum, at $y/d \approx 0.9$. We can assume that the amplitude of the vortex street is reduced in this case by way of interference with the jet emanating form the gap between the two solids.

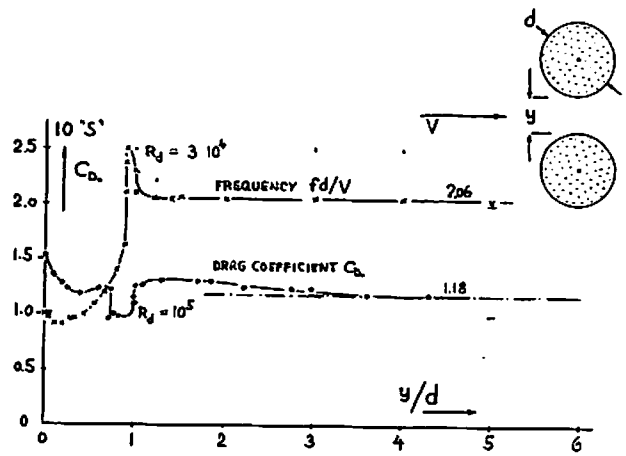


Figure 5. Drag (2,a) (and vortex-street frequency, reference 2,b) of a pair of circular cylinders placed side by side.

Pair Of Struts. Past the sides of round or streamline shapes, the average velocity (just outside the boundary layer) is always increased. In case of the pair of strut sections in *figure 6*, the positive pressure gradient along the rear, automatically associated with that increase of velocity, is evidently responsible for a considerable increase of the drag coefficient, particularly below $y/t = 1$. The two sections form a nozzle between them whose expansion ratio increases as their lateral distance is reduced. The flow through this nozzle separates as the clearance approaches zero.

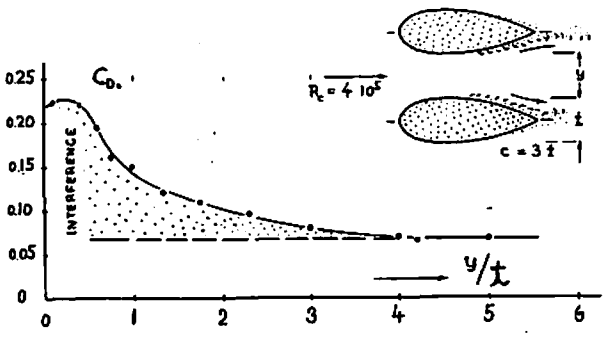


Figure 6. Drag of a pair of struts, one beside the other (2,a).

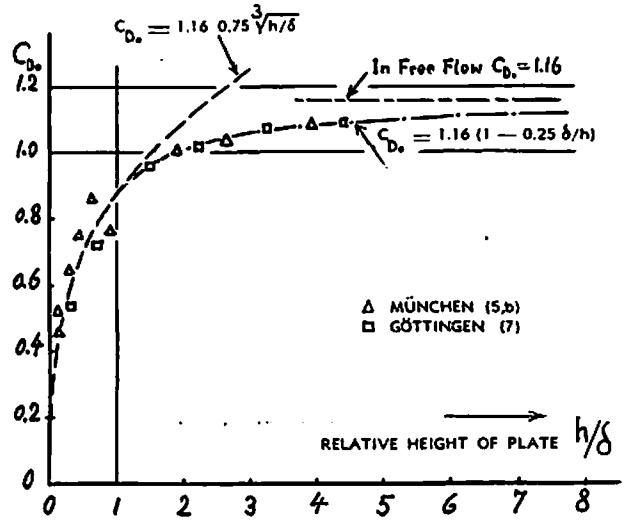


Figure 7. Drag coefficient of square plates attached to a plane wall, as a function of their height in comparison to boundary-layer thickness.

(1) Interference between bodies one behind the other:
a) Eiffel, La Résistance de l'Air, Paris 1914.
b) Lange (DVL), Antenna Rods. ZWB UM 1238 (1944).
(2) Drag of pairs of solids:
a) Biermann and Herrnstein, Interference Between Struts in Combinations, NACA T.Rpt. 468 (1933).
b) Vortex Frequency, J.Aeron.Sci. 1946 p.289.
(3) Drag of spheres affected by supporting devices:
a) Hoerner, Experiments with Spheres (Brunswick and DVL), Luftfahrtforschung 1935 p..42.
b) ARC, Wind-Tunnel Turbulence, RM 1662 (1934).
c) Bacon-Reid, Spheres, NACA T.Rpt 185 (1928).
d) Nat.Luchtvaart Lab. Amsterdam Rpt A.950 1947.
(5) Engelhardt, Aerody. Laboratory TH München:
a) Fuselage-Tail Interference, Rpts 1 and 3/1943.
b) Drag of Half Bodies on Walls, Rpt 5/1943.
c) Interference on Tail Surfaces, Rpt 4/1943.
d) Hoerner, Influence of Fuselage on Tail (5,a), Messerschmitt Rpts TB 54/1942 and 88/1943.

2. DRAG OF HALF BODIES ON WALLS

The drag of bodies attached to plane (or other) walls, is similar to that of surface protuberances as presented in Chapter V. In comparison to them, the size of the half bodies considered in the following paragraphs is usually much larger, however. This is especially true of aircraft appendages, such as canopies, armament turrets and similar component parts, which may be added to the outer surface of fuselages or wings.

Effective Dynamic Pressure. As a simple case, the drag of a small plate or disk is considered first, attached to a plane wall. Plates in three-dimensional flow have a comparatively constant flow pattern; and their drag adjusts itself to the local average or effective dynamic pressure to which they are exposed. For plate sizes, small in comparison to the thickness of the boundary layer, the effective dynamic pressure is given in equation 9 of the chapter on "surface imperfections". Considering, however, bodies which are higher than the boundary layer, only their bottom is exposed to reduced dynamic pressure. The loss of momentum can, therefore, be considered to be concentrated in a thin sheet. In turbulent flow, the thickness of this sheet is in the order of $y/\delta = 0.25$. Hence the effective dynamic pressure:

$$q_e/q_f = 1 - 0.25\,(\delta/h) \qquad (1)$$

Figure 7 confirms this calculation. Based upon the effective dynamic pressure, circular and square plates, attached to a plane wall, show "independent" drag coefficients c_{D_o} which (on the average) are of the same magnitude (≈ 1.17) as known under free-flow conditions. An average rough value for the thickness of the boundary layer originating along the surface of aircraft (including some surface imperfections) is

$$\delta \approx 0.02\ x; \quad \text{or} \quad \delta/x \approx 2\% \qquad (2)$$

with x = distance from the stagnation point of the respective body to the point where the plate (or any other part) is attached. Combining equations 1 and 2,

$$q_e/q_f = 1 - 0.005\,(x/h) \qquad (3)$$

Two Dimensional Plates. In the case of *two-dimensional* plates (strips) or similar protuberances, the formation of a vortex street is possibly prevented by the wall to which these bodies are attached. As found in (7), their drag coefficient is therefore in the order of $c_{D_o} = 1.25$, instead of 1.97 as found in free flow.

3. DRAG OF FLOATS AND BOAT HULLS

In regard to their aerodynamic drag, flying-boat hulls, and floats are similar to fuselages. However, since their lower side is specifically designed for the purpose of taking off from, and landing on water — the drag of these bodies is somewhat higher than that of comparable streamline or fuselage bodies.

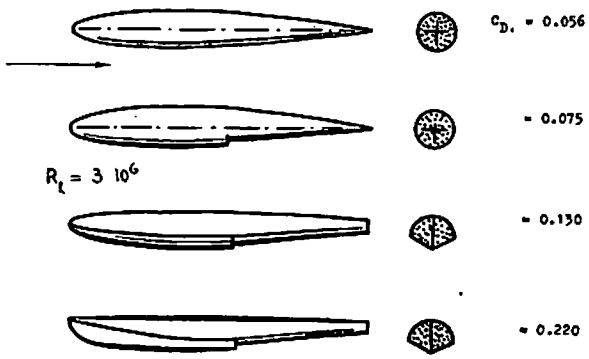


Figure 22. Drag of a float (12,a) developed from a basic streamline body by adding step and chines.

Chines. Figure 22 shows how the aerodynamic drag of a float growth upon developing its final shape from that of a basic streamline body of revolution. It is seen that the addition of the sharp chines (needed to make the bottom effectively planing on the water) increases the drag appreciably. Because of the sharp deck line in their forebody, the drag coefficient of floats can be several times as high as that of the basic body. A well-rounded deck (in the third shape of figure 22) may keep the drag within acceptable limits, however. *Figure 23* proves that the drag increment due to chines is comparatively less in flying-boat hulls.

(12) Aerodynamic drag of seaplane floats:
- a) Diehl, Navy Yard, "Engineering Aerodynamics".
- b) Cowley, Model Tests for "Schneider Trophy" Contest, ARC RM 1296 through 1299 (1928).
- c) Floats and Boats, Luftwissen 1939 p.101.
- d) NACA, Full Scale, W.Rpt L-238, presents Coefficients between C_{D_o} = 0.15 and 0.21; C_{D_Δ} = 0.04 and 0.06.

(13) Aerodynamic drag of flying boat hulls:
- a) Smith and Allen, Review on Flying Boats, including data from NACA T.Notes 1305 to 1307 and 1686, T.Rpts 766 and 1144; ARC RM 2896 (1954).
- b) Aerodynamics and Hydrodynamics, NACA T.Rpt 766.
- c) Riebe and Naeseth, Refined Flying Boat Hull, NACA Tech Note 2489 or Tech Rpt 1144.

(14) Drag of steps on seaplane hulls:
- a) Hartman, NACA Technical Note 525 (1935).
- b) Diehl, NACA T.Rpt 236; also quoted in his "Engineering Aerodynamics" p.290.
- c) See results on floats in reference (12,b).
- d) Hamilton Flying Boats, ARC RM 2899 (1956).
- e) ARC Rpts: RM 2708 (1945) 2834, 2896 (1955).
- f) NACA, Tech. Notes 1307 (1947) and 2762 (1952).

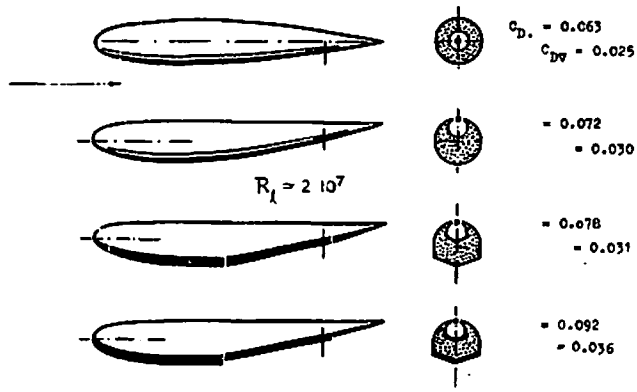


Figure 23. Drag of flying-boat hull (14,a), developed from streamline body having same length and same displacement.

Fineness Ratio. Figure 24 presents the drag coefficient (on frontal area) of a series of smooth seaplane hull models as a function of their fineness ratio (defined in equation 1). The optimum ratio with respect to drag on frontal area, seems to be in the vicinity of 5. Based on $(\text{volume})^{2/3}$, a minimum drag coefficient is obtained at l/"d" $\approx$ 9, corresponding to l/b $\approx$ 13 in the hull family tested. Modern development of flying boats tends toward comparatively high length/beam ratios, up to 20 or even higher (not to be confused with the l/"d" ratio). A considerable increase of the height ratio (h/b) to the order of 3 and higher goes hand in hand with that development; and this increase makes wetted area and frictional drag larger than those in a comparable streamline body of revolution.

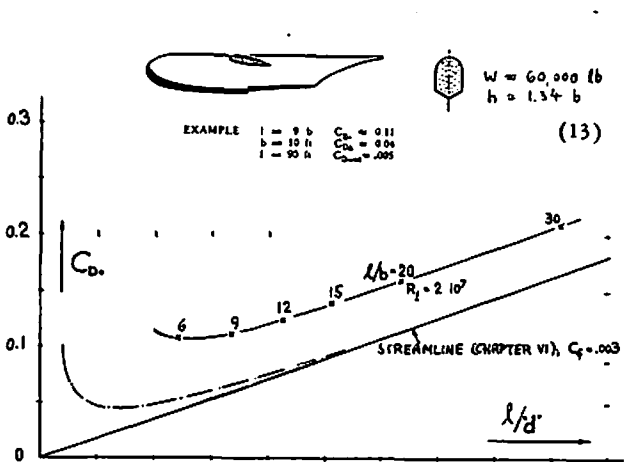


Figure 24. Drag coefficient of a series of flying-boat hulls as a function of their fineness ratio l/"d".

Steps. Steps cut into the lower side of floats and flying boats are necessary to break the suction of the water, and to keep the airplane balanced at angles of attack desirable for short take-off. The drag of these steps, plotted in *figure 25*, can be calculated in

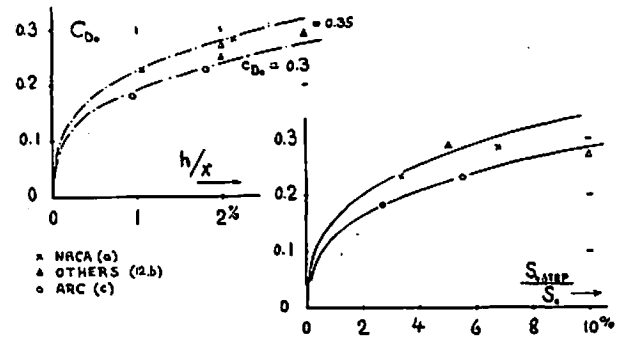


Figure 25. Drag coefficient of and due to steps (14) in the bottom of floats and flying boats; (a) as a function of height ratio (x = distance from nose) and (b) against frontal area ratio.

a way similar to that of sheet-metal joints. Selecting from the material presented in Chapter V, an "independent" coefficient $c_{D_s} = 0.2$, the drag coefficient of steps (based on frontal step area) is suggested to be

$$C_{D_s} = 3\sqrt[3]{(h/x)}\ 0.2 = 0.6\sqrt[3]{(h/x)} \qquad (8)$$

where h = height of step and x = distance between body nose and step. Drag coefficients in figure 25, recalculated from experimental results on floats and hulls, are some 50% higher than the theoretical value. The increment is evidently caused by interference originating behind the step along the rear of the boat body. Part "b" of figure 25 presents the same drag coefficients as a function of the frontal area ratio.

Step Fairing. During flight, the step is not needed. By deflecting a flap or by any other mechanism, the step may therefore be faired, after taking off. *Figure 26* (shape "c") shows that most of the step drag can be eliminated in this way. The attempt shown as number "b", "streamlining" the step in the plan form, is not very successful. Another method of eliminating the step drag is proposed in (13,c). Both body and bottom of the hull terminate together in a vertical edge, while the afterbody is replaced by a "boom", high in the air. The low drag coefficient of this type hull (in the order of $C_{D_s} = 0.045$) is also brought about by elimination of wetted area.

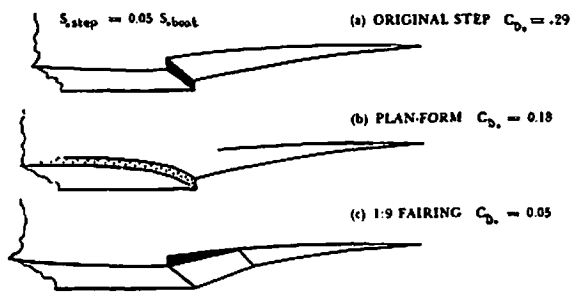


Figure 26. Variation of step drag coefficient due to shape and fairing (14,d).

4. DRAG OF LIFTING SURFACES

Principles of drag due to lift are presented in the "lift" chapter; and the parasitic drag of airfoil sections is treated in the "streamline" chapter. All that is left to be considered here is, therefore, a number of supplementary items (such as the drag of tail surfaces) and the drag caused by devices such as brake flaps.

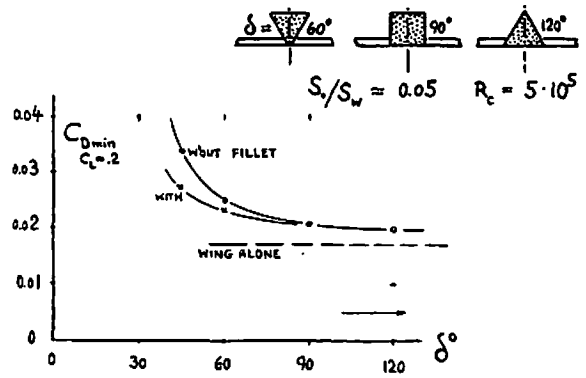
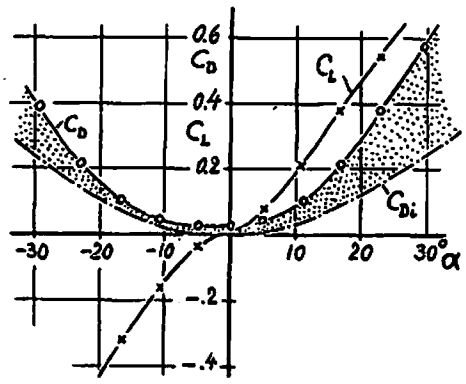
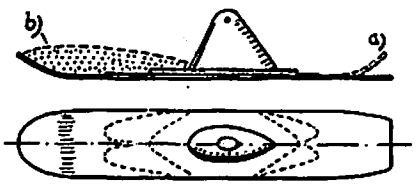


Figure 27. Drag of a wing-fuselage configuration as a function of the angle along the wing roots (15).

Interference Drag. The parasitic interference along the wing roots is among others a function of the angle in the corner between wing and fuselage wall. *Figure 27* shows that the drag increases considerably as the angle δ is decreased below some 90° . — The extensive and systematic investigations in (16) have often been quoted and evaluated, showing the influence of shape, relative position and that of fairings (fillets) upon the drag of wing-fuselage combinations. Interference is, of course, particularly strong at higher lift coefficients. *Figure 28* shows the variation of the parasitic drag (obtained after subtracting $C_{D_i} = C_L^2/\pi A$) at a lift coefficient $C_L = 1$, as a function of the vertical location of wing against fuselage. The lowest drag is obtained in mid-wing arrangement (or slightly above) where 15% of the wing area is covered by the fuselage body. The parasitic interference drag is largest in low-wing condition, where an expanding passage is formed between fuselage and the rear of the wing's suction side. A lesser peak of interference drag is found in the high-wing configuration. Both the high-wing and particularly the low-wing drag can appreciably be reduced by means of suitable fillets, design instructions for, and aerodynamic characteristics of which are given in (16).





DRAG COEFFICIENTS ON PLAN-FORM ----- AREA:
MINIMUM: $C_D = 0.03$
DUE TO (a) $\Delta C_D = +.07$
DUE TO (b) $\Delta C_D = -.02$

Figure 40. Aerodynamic lift and drag characteristics of an airplane ski (26).

Skis. Airplane skis present aerodynamic characteristics similar to those of "wings" of extremely small aspect ratio (see in Chapter VII). The aspect ratio of the ski in *figure 40* is, for example, $A = b^2/S = 0.19$ only. The drag due to lift corresponding to this ratio, determined through the use of the equations presented in the chapter mentioned, is considerable in comparison to the minimum parasitic drag of such a ski.

6. DRAG OF EXTERNAL LOADS

Loads which cannot readily be stowed within fuselage or wing of airplanes, or which are to be dropped during the flight (bombs) are attached to the outside of aircraft. Their drag is twofold; they have a drag of their own and they cause some interference drag.

Streamline Tanks, employed to carry additional fuel, have usually the shape of streamline bodies. Originally, such tanks were sometimes attached to existing bomb racks, primarily under the wings. Number "j" in figure 41 shows that their drag is comparatively high in this condition ($C_{D_o} = 0.26$), evidently because of interference effects within the narrow spaces between wing, supporting parts and tank. The purpose of such tanks, to increase the range of the airplane, is thus curtailed to a considerable extent by the added drag. Fairing the bomb rack by means of a sheet-metal collar, somewhat reduces the drag coefficient (see number "i" with $C_{D_o} = 0.13$). The "neck" is obviously too thick in this case, however. The most favorable method of carrying a tank underneath the wing, is that on a streamline pylon (number "n" in figure 41). *Figure 42* shows the drag added by the presence of the pylon (increasing with its length); and it indicates one component of interference drag between tank and wing which decreases to zero as the clearance distance is increased to and beyond y/d = o.5. Including the pylon drag, the minimum is found in the vicinity of y/d = 0.2 or 0.3 for two of the configurations investigated and in the order of 0.5 for the others. Experimental results in (30,n) indicate that in this type of suspension, tank locations under or ahead of the wing's leading edge (such as they are applied in modern jet engine nacelles) are very favorable (giving drag coefficients in the order of $C_{D_o} = 0.05$, including pylon and interference).

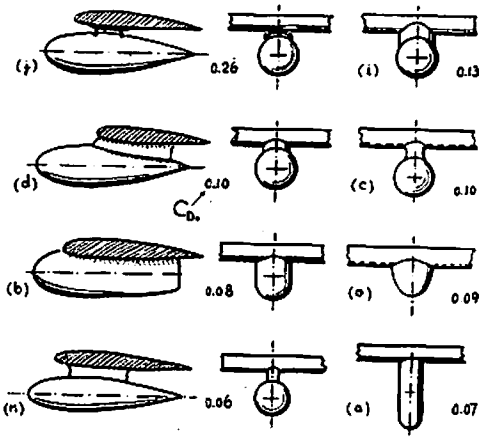


Figure 41. Shape and drag coefficient of various external stores (tanks) mounted under the wing (30).

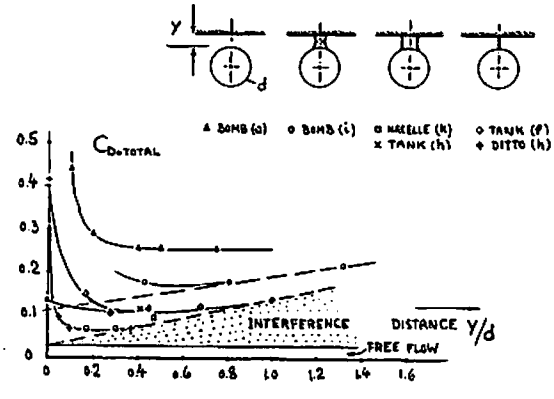


Figure 42. Drag coefficients of several tanks (and bombs) suspended by means of a neck or pylon underneath a wing (30), as a function of the clearance ratio y/d.

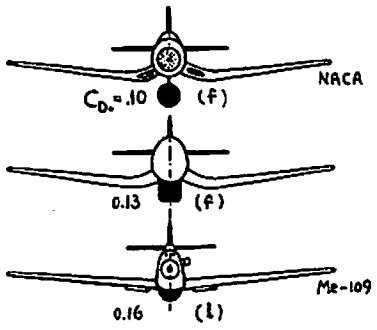


Figure 43. Examples of external tanks under the fuselage of low-wing airplanes (30).

"Belly" Tanks. A "belly" type tank, mounted under the fuselage of the Me-109 is analyzed in Chapter VIII, having a coefficient $C_{D_o} = 0.16$. In addition to this tank, *figure 43* presents three arrangements under the fuselage of fighter airplanes, two of them in "belly" form. It is seen that suspension by means of a "pylon" yields a smaller drag coefficient. Generally, the place under the fuselage of low-wing airplanes, does not appear to be very favorable, however, to attach an external tank. Figure 41 "e" shows a "belly" shape mounted under a wing with a drag coefficient of 0.09. Increasing the height to breadth ratio of such tanks, a "nacelle" type is obtained as in "b" of the illustration. Further modifications of this type are reported in (30,a). Minimum drag is found in a shape having a height ratio in the vicinity of h/b = 5, approximately as in "a" in figure 41. However, because of its foil-like form, developing lateral forces, such a tank may not be very desirable.

Streamline Arrangements at the upper side of the wing are presented in *figure 44*. The second form, a low-wing nacelle-type tank, has of course an induced drag component similar to that of "b" or "e" in figure 41. Shifting, however, such a tank to the rear, and giving it a flat and wide "beaver tail" pointing *upward* (thus eliminating the induced drag component), the lowest drag coefficient ($C_{D_o} = 0.03$) is obtained among all arrangements quoted.

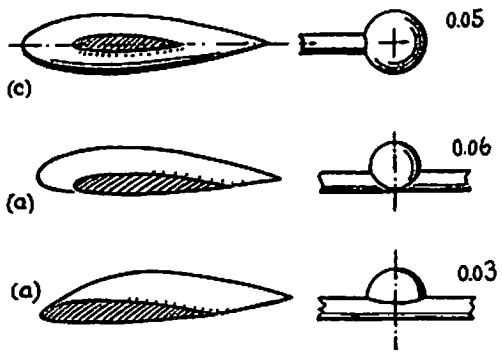


Figure 44. Drag coefficients of tanks (31) attached to the upper side or at the tips, respectively, of wings.

Wing-Tip Tanks. Many modern fighter planes and some other airplanes are equipped with wing-tip tanks. Their influence on effective aspect ratio and induced drag is discussed in the "lift" chapter. Regarding their parasitic drag (at small to moderately large lift coefficients), shape "c" in figure 44 indicates a drag coefficient in the order of $C_{D_o} = 0.05$.

Range. For illustration, a small fighter airplane may be considered with a "drag area" at cruising speed, $f = D/q = (C_D \cdot S) = 8$ ft^2 and a regular fuel load "F" = 200 gallons. Through addition of a pair of external tanks with a total of Δ'F' = 200 gallons of fuel, the range of this airplane may theoretically be increased by 100%. Actually, the tanks increase the drag area by $\Delta f = C_{D_o} S_o$. Consequently, with "R" denoting the range of the airplane under specified conditions,

$$\frac{R + \Delta R}{R} \approx \frac{1 + (\Delta F/F)}{1 + (\Delta f/f)} \qquad (15)$$

Assuming in the considered example a frontal area of each tank $S_o = 2$ ft^2, the range is increased to only ≈ 1.77 times the original value, for an unfavorable tank drag coefficient of $C_{D_o} = 0.26$ (as in figure 41,j). With the most favorable coefficient listed in figure 44 ($C_{D_o} = 0.03$), the range ratio is 1.97, which is essentially equal to the value simply corresponding to the number of gallons aboard.

(30) Drag of external stores (tanks) under aircraft:
- a) Russian Catalog, Bombs and Stores, Moscow 1940.
- b) Dornier, Do-217 External Tanks, Rpt 74, 1940.
- c) Dornier, Do-217 Flight Test with Tank, 1940.
- d) Me-264 Wind Tunnel Tests Rpt AVA 42/W/34.
- e) Owen-Becker-Nogg, Tanks, RAE Rpt 8146.
- f) Pepper, Auxiliary Tanks, NACA W.Rpt L-371.
- g) RAE, Drop Tanks on Swept Wing, ARC RM 2951.
- h) Junkers, Wind-Tunnel Tests on External Tanks Ju-288, Rpts D.6372 and 6633 (1939/40).
- i) Messerschmitt, 109 Flight Tests, Rpt 16/L/1943.
- k) Wiesener, Force- and Pressure-Distribution on Combination of Wing with Tank, ZWB Rpt UM 1090 (1943).
- l) Hoerner, The Drag of Bombs Hung from the Outside of Airplanes, ZWB Rpt UM 7814 (1943).
- m) Arado, Pair of Jet-Engine Nacelles, LFA 1943.
- n) Silvers and Spreemann, NACA RM L7K20 (1947).
- o) Pylon tanks also in NACA RM L50L12 and L51D26.

(31) External stores at upper side and at tips of wing:
- a) Hütter, External Store "Doppelreiter" on Upper Side of Wing, Document ZWB UM 4592, 1944.
- b) NACA, Wing-Tip Tanks, RM A5F02 and L9J04.
- c) Messerschmitt, Tip Tank, Darmstadt 1943.

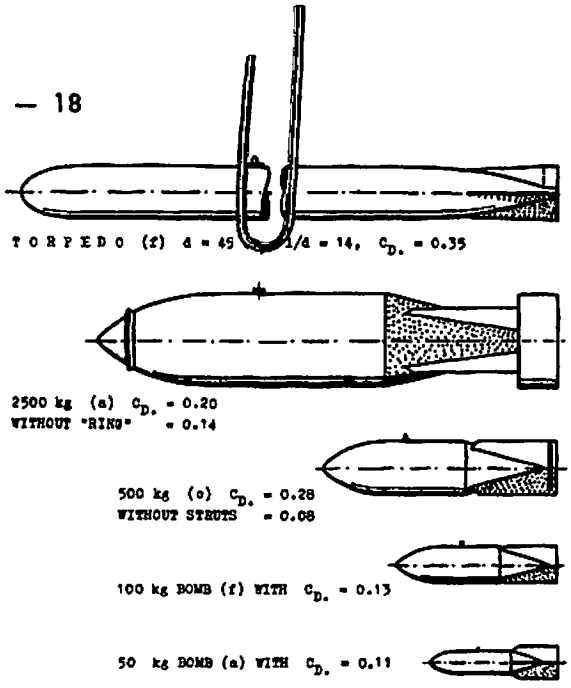


Figure 45. Drag coefficients of bombs and of one torpedo (32) in free flow (at subcritical speeds).

Bombs as such are treated in the "transonic" chapter. In this section here, bombs are primarily considered being carried on the outside of airplanes. Inasmuch as this application is restricted to subsonic speeds, the drag of bombs is presented without accounting for any effects of compressibility. The drag coefficients of bombs in free flow, listed in *figure 45*, are several times as high as those of comparable streamline bodies. The additional drag is caused by the comparatively bluff shape as well as by fins and other protuberances, such as attachments needed to support bombs under the wing or the fuselage of an airplane. The drag coefficient is at least $C_{D_o} = 0.09$. Bombs with the fins stiffened by means of round struts show values up to $C_{D_o} \approx 0.3$. The additional drag due to a nose ring (favorable to get such a bomb *into* water at the side of ships) is $\Delta C_{D_o} = 0.05$. The drag coefficient of aircraft torpedos corresponds to their length. Figure 45 shows a tested value of $C_{D_o} = 0.35$.

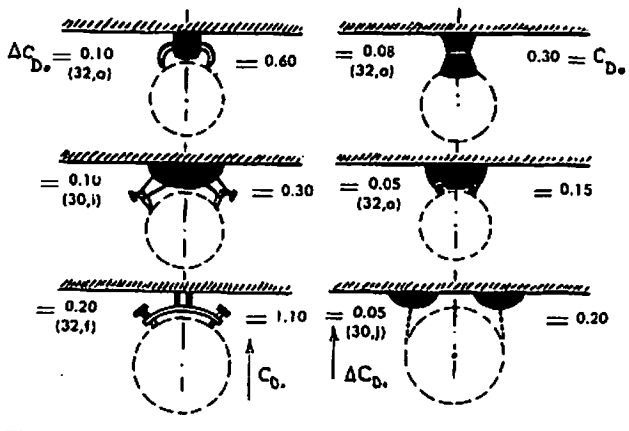


Figure 46. Drag of several bomb racks (and similar devices). The coefficients, of the racks as well (ΔC_{D_o}) and those of the complete configuration (with bombs attached, indicated by C_{D_o}), are based in each case upon the respective bomb's frontal area.

Bomb Racks. In order to support a bomb and to keep it safely in place, a rack is needed. After dropping the bomb, the rack usually remains exposed to the air stream. The drag of such racks is comparatively high. Based on frontal area of the bomb which the rack is designed to carry, *figure 46* shows drag values which are in the same order as those of the bombs themselves. The drag of the protruding parts can be estimated on the basis of their frontal area and the following drag coefficients:

for streamline fairings around rack $C_{D_o} = 0.1$
for arms (rods and other blunt parts) $C_{D_o} = 1.0$

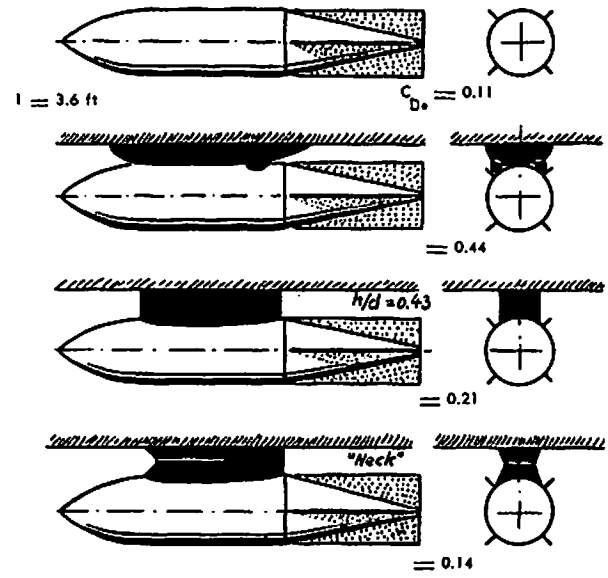


Figure 47. The drag coefficient of a 50 kg bomb (32,a) in combination with various racks or necks, respectively.

Neck Suspension. Figure 47 shows several methods of suspending a bomb under a wing or fuselage. The additional drag of a bomb rack and due to the interference between this rack, the bomb and the wing, is in the order of $\Delta C_{D_o} = 0.3$. The most favorable type of suspension is by means of a neck or pylon; the minimum drag increment caused by such an arrangement corresponds to only $\Delta C_{D_o} = 0.03$.

Interference Drag. Basically, bombs (with higher drag coefficients) cause an interference drag which is larger than that due to tanks (having lower drag coefficients). In regard to the angular position of bombs (or tanks) against the lower side of the wing (or the fuselage respectively), the smallest total drag is found in the vicinity of $\Delta\alpha = -3°$ (measured against wing chord); that is, with the tail of the bomb somewhat closer to the adjoining wing side than with the nose. If placing two or more bombs (or nacelles or external stores) closely beside each other, their drag may be increased because of mutual interference.

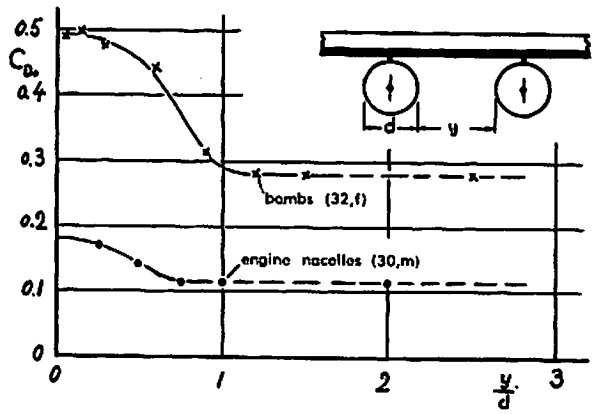
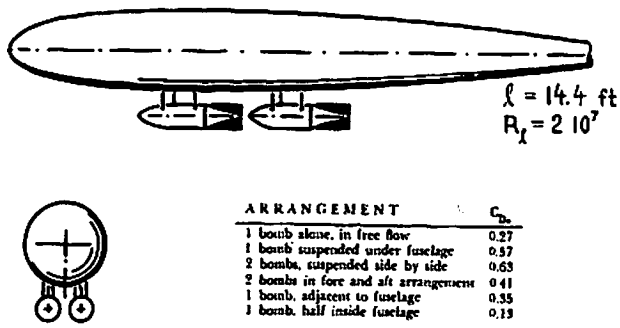


Figure 48. Drag coefficients of pairs of bombs and tanks (or nacelles), respectively, as a function of their lateral distance.

However, beyond a lateral distance of approximately e = d, *figure 48* does not show interference any longer. Placing, on the other hand, two bombs behind each other, their total or average drag coefficient is reduced; as can be seen in *figure 49*. Within the wake of the forward bombs, the drag of the rear bombs is evidently smaller than in unobstructed flow.



ARRANGEMENT	C_{D_0}
1 bomb alone, in free flow	0.27
1 bomb suspended under fuselage	0.57
2 bombs, suspended side by side	0.63
2 bombs in fore and aft arrangement	0.41
1 bomb, adjacent to fuselage	0.35
1 bomb, half inside fuselage	0.13

Figure 49. Drag of bombs in several arrangements, suspended under the fuselage of an airplane (32,e).

7. DRAG OF MISCELLANEOUS PARTS

(a) Drag Of Cylindrical Parts

Drag characteristics of circular (and other) cylinders are treated in Chapter III, as a function of Reynolds number, surface roughness and angle of inclination. Certain applications in aircraft are discussed as follows.

Fairings. Gun barrels sticking out of bombers, in directions crosswise to the air flow, present considerable drag due to their cylindrical shape, particularly in the range of Reynolds numbers below transition. These drag forces may also curtail handling and aiming of the guns, because of the moment about the center of their rotation. *Figure 50* shows some attempts of reducing the drag of cylindrical bodies by adding fairings to their rear side. The results are small, however; the gap in the surface between cylinder and fairing, and the bluff shape of the half-cylindrical nose, evidently prevent the flow from getting sufficiently far attached to the rear of the fairings. Similar results are obtained using sleeve-type fairings, presented in *figure 51*. Sleeves can be attached in such a manner that they adjust themselves automatically to the direction of the air flow when applied to gun barrels or other aircraft equipment. By increasing the chord of the fairing and/or by thickening the trailing edge (as described in Chapter III) it is furthermore possible to increase the critical Mach number (see Chapter XV) from ≈ 0.55 to ≈ 0.70 in the shapes presented in figure 51.

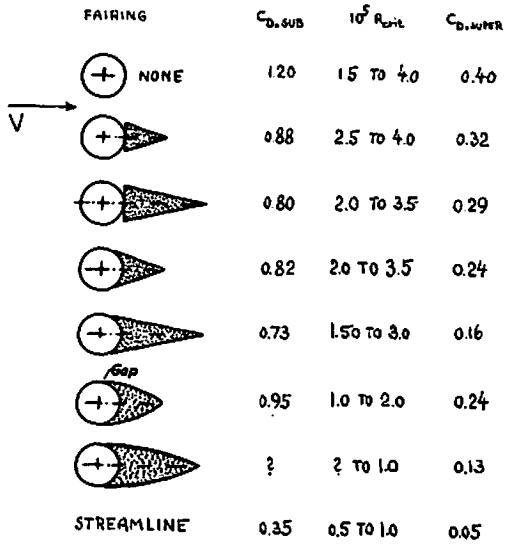


Figure 50. Influence of various fairings on drag of circular cylinder (35,a), at R'numbers above transition.

(32) Drag of bombs, attached to aircraft:
- a) Heinrich, Wind-Tunnel Investigation of Wing with Bombs, ZWB UM 4574 (FGZ 1944); Transl by Cornell Aeron.Lab 1949.
- b) Arado, Wind-Tunnel Investigation of a Pair of Jet Engines at the LFA Brunswick 1943.
- c) Göthert, Investigation of Bombs SC-50, -250, -5000, Document ZWB FB 1663.
- e) Kosin, Fuselages, Yearbk D.Lufo 1942 p.I,241.
- f) Russian Bomb and Tank Catalog (30,a).
- g) Hoerner, Bombs, Messerschmitt Rpt TB 85/1943.
- h) Stoney-Royall, Smooth Shapes, NACA RM L56D16.
- i) NACA, Full-Scale Bombs, W.Rpt L-131 (1944).

(35) Means of reducing drag of circular cylinders:
- a) Kramer, Unpublished DVL Tests, 1934.
- b) Junkers, Sleeve-type Fairings in Junkers High-Speed Tunnel, Rpts S.1943/85 and S.1944/13.
- c) Guide Vanes for Periscopes, TMB Rpt 504 (1945).